On the Effects of Predeformation on Work Hardening of Ultra-Low-Carbon Sheet Steel

R.A. Mirshams, H.P. Mohamadian, and K.E. Crosby

Predeformation affects the work-hardening behavior of sheet metals in sequential forming operations by producing various strain histories in different parts of the sheet. Several investigators have reported the effects of two-stage deformation on the behavior of sheet metals, particularly justification has been presented on face-centered cubic (fcc) alloys. However, the works on low-carbon ferritic steels are not conclusive. This article reports some new findings of the effects of two modes of predeformation on the subsequent stress-strain relationship in ultra-low-carbon sheet steels. The details of a laboratory test system are presented along with methods used to reduce the data. The effect of the stability ratio, a measure of the degree to which the interstitial atoms are free, on the hardening rate at second-stage of deformation was studied. For stabilized sheet steels, it was found that changes in strain path from equibiaxial stretching to uniaxial tension cause an increase in the flow stress relative to the flow stress at similar effective strain in continued monotonic. For unstabilized sheet steels, a significant increase in the flow stress was not observed with either equibiaxial prestraining or cold rolling and equibiaxial stretching.

Keywords
Low carbon steel, sheet forming, work hardening

1. Introduction

THE effects of predeformation on the work-hardening behavior of sheet metals in sequential operations are of utmost importance in sheet forming. These processes produce various strain histories in different parts of sheet metal. The effects of strain path on work-hardening behavior influence the limit of useful strain to the final shaping processes. This article reports some new findings on the effects of two predeformation modes on the subsequent stress-strain relationships in uniaxial tension on ultra-low-carbon sheet steels.

Wagoner and Laukonis[1] summarized noticeable features of other investigators on the effect of two-stage deformation on the behavior of sheet metals in the introduction of their paper. They investigated the effect of plane-strain deformation in the first-stage on work-hardening behavior in the subsequent uniaxial tensile tests on aluminum-killed steel. They concluded that no major differences in mechanical properties were found between sheet prestrained by rolling and plane-strain tension. However, their results showed a significant effect of the direction of subsequent tensile tests to the direction of the first-stage plane-strain deformation.

In a more recent work, Zandrahimi et al.[2] gave comparisons of the effect of strain path and history on the work-hardening behavior of 70/30 brass, low-carbon steel, aluminum, copper, and two austenitic steels. They pointed out that fcc alloys of low stacking fault energy (SFE) were less susceptible to the reduction of work-hardening rate than low-carbon ferritic steels. On the other hand, they also referred to the influence of microstructural features such as grain size, crystallographic texture, and factors that mainly affect flow stress in the early stages of plastic deformation, such as apparent latent hardening and residual stress. Recently, Doucet and Natarajan[3] reported an experimental study on the yielding behavior of interstitial free (IF) steel and 70/30 brass that they prestrained in plane strain and subsequently strained in uniaxial tension. In this study, the yield point was defined using the axial strain versus the transverse strain curve, as measured with biaxial resistance strain gages, during the second-stage test. Their measurements indicated that prestrained brass and steel both yielded at stresses lower than the expected monotonic levels; however, they did not give an explanation for this observation. This article presents some new findings on the effects of two modes of predeformation on the subsequent stress-strain relationship in ultra-low-carbon sheet steels.

R.A. Mirshams, H.P. Mohamadian, and **K.E. Crosby,** Department of Mechanical Engineering, Southern University, Baton Rouge, LA. 70813.

2. Experimental Procedure

2.1 *Material*

Ultra-low-carbon sheet steels with a chemical composition as summarized in Table 1 were selected. The difference between the two types of sheet used in this study was the calculated stability ratios. Stability ratio (SR), a measure of the degree to which the interstitial atoms are free, is calculated by the following relationship:

$$SR = \frac{[Nb] / 92.9 + \{[Ti] - 48 / 32[S] - 48 / 14[N]\} / 47.9}{[C] / 12.01}$$

where [ ] is weight percent of the alloying element.

A calculated value of SR > 1 implies there are no free interstitials, and the steel is thus referred to as stabilized; SR < 1 refers to an unstabilized steel. To examine the effect of aging on strain hardening, specimens from both sheet materials were prestrained uniaxially, heat treated at about 200 °C for 30 min, and cooled to room temperature. Figures 1(a) and (b) present through-thickness microstructures of the stabilized (S) and un-

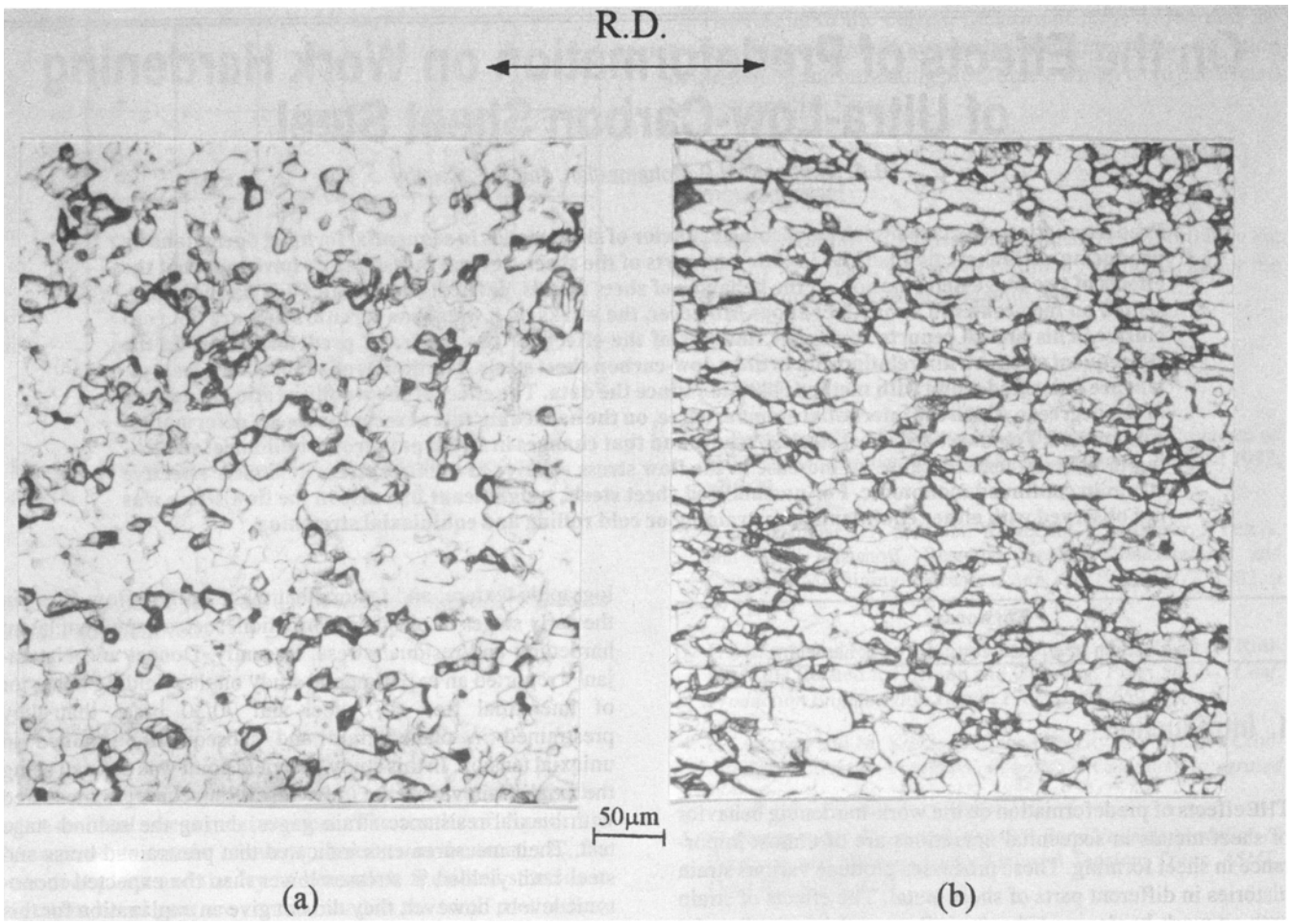

Fig. 1 Optical micrograph of through-thickness microstructure of stabilized (a) and unstabilized (b) sheet steel, 3% nital etchant.

Table 1 Compositions of sheet steels

	Composition, wt%														
Steel	C	S	Mn	P	Si	Cu	Ni	Mo	Cr	Nb	Ti	Al	Sn	N	SR
Stabilized (S)	0.0033	0.009	0.19	0.011	0.016	0.01	0.01	0.01	0.01	<0.008	0.099	0.053	0.01	0.0071	4.65
Unstabilized (U)	0.0042	0.006	0.19	0.009	0.013	0.01	0.01	0.01	0.01	<0.008	<0.002	0.079	0.01	0.0043	<0

stabilized (U) steel sheet. Standard metallography procedures were applied for specimen preparation, and a 3% nital solution was used for etching.

2.2 *Biaxial Stretching and Cold Rolling*

In-plane biaxial stretching was performed by using a flat-bottomed punch. This type of test is known as the Marciniak biaxial stretching test, and detailed information can be found in Ref 4. Rectangular blanks of the ultra-low-carbon sheet steels were stretched over a flat-bottomed punch with cylindrical cross section of 10.16 cm (4 in.) in diameter. The center of the punch was hollowed out to eliminate friction in the central area with a diameter of approximately 7.62 cm (3 in.). Oil was used as a lubricant to reduce friction. The punch speed was kept constant during stretching of the different specimens. Testing was carried out on a punch and die setup that had been installed on an MTS servohydraulic system in the Department of Metallurgical and Materials Engineering, Colorado School of Mines (CSM). Cold rolling was performed in the materials processing laboratory at CSM. Table 2 presents the prestraining matrix.

2.3 *Mechanical Testing and Data Analysis*

Tensile test specimens were cut parallel and transverse to the rolling direction and stretched uniaxially by a servohydraulic Instron machine (model 1230) with a constant crosshead speed of 2.54 mm/min (0.1 in./min). A 12.7-mm (0.5-in.) gage extensometer was used to record extension, and the tests were performed in the stroke control mode. An interactive data acquisition system was used to collect and transfer data to a personal computer. A spreadsheet software program

Table 2 Prestraining matrix for experiments on ultra-low-carbon sheet steels

Prestraining conditions/ material	Uniaxial prestrain + aging, ε (a)	Equibiaxial prestrain, ε (a)	Cold rolling + equibiaxial prestrain, ε (a) ($\varepsilon_R + \varepsilon_B$)	Equibiaxial prestrain, ε (a)
S-RD (b)	0.095	0.082	0.035 + 0.035	0.05
S-TD (b)	0.095	0.083	0.035 + 0.035	0.05
U-RD (b)	0.10	0.090	0.05 + 0.06	0.17
U-TD (b)	0.10	0.090	0.05 + 0.06	0.14

(a) $\varepsilon = \ln (t/t_o)$, where t = sheet thickness after prestrain; and t_o = original sheet thickness. The noted figures are the average of six measurements; ε_R and ε_B refer to true thickness strains for rolling and biaxial straining. (b) RD and TD refer to the rolling and transverse directions.

was used to make the necessary conversions and calculations. The data were smoothed with a graphics software package that used the following procedure: (1) sorting data by X-value and removing duplicate X-values, (2) removing any linear trend from the data, (3) low-pass filtering by using Fast Fourier Transformation (FFT) to average approximately five points, and (4) reversing the data transformation and reinserting the linear trend. The smoothing procedure was applied at least three times on each set of data.

3. Results and Discussion

The results in this section graphically represent the relationships between the total effective true strain (ε) and the flow stress (σ) in a ln-ln scale. Each true stress/true strain curve is representative of an average of at least two tests. The levels of effective prestraining and effective stress and strain curves were calculated using Von Mises criterion with allowance for the effects of anisotropy by applying Hill's analysis. Assuming planar anisotropy, the effective stress, σ_e, and strain increment, $d\varepsilon_e$, in a biaxial stress state are given by

$$\sigma_e = \sqrt{\frac{3(1+\bar{R})}{2(2+\bar{R})}} \left\{ 1 + \left(\frac{\sigma_2}{\sigma_1}\right)^2 - \frac{2\bar{R}\left(\frac{\sigma_2}{\sigma_1}\right)}{(\bar{R}+1)} \right\}^{1/2} \sigma_1 \qquad [1]$$

$$\varepsilon_e = \sqrt{\frac{2(1+\bar{R})(2+\bar{R})}{3(2\bar{R}+1)}} \left\{ 1 + \left(\frac{\varepsilon_2}{\varepsilon_1}\right) + \frac{2\bar{R}\left(\frac{\varepsilon_2}{\varepsilon_1}\right)}{(\bar{R}+1)} \right\}^{1/2} \varepsilon_1 \qquad [2]$$

and

$$\frac{\sigma_2}{\sigma_1} = \frac{(1+\bar{R})\left(\frac{\varepsilon_2}{\varepsilon_1}\right) + \bar{R}}{1 + \bar{R} + \bar{R}\left(\frac{\varepsilon_2}{\varepsilon_1}\right)}$$

where σ_1 and σ_2 are the principal stresses; ε_1 and ε_2 are the principal strains that lie in the sheet directions. $\bar{R}$ is the average plastic anisotropy parameter, which is normally calculated from

$$\bar{R} = \frac{R_{0^\circ} + 2R_{45^\circ} + R_{90^\circ}}{4}$$

The subscripts identify the test directions with reference to the rolling direction. The R-value for each direction is defined in terms of true strain, ε, in the length, l, width, w, and thickness, t, of the gage length of a tensile test piece:

$$R = \frac{\varepsilon_w}{\varepsilon_t}$$

Assuming constancy of volume

$$\varepsilon_l + \varepsilon_w + \varepsilon_t = 0$$

$$R = -\frac{\varepsilon_w}{(\varepsilon_l + \varepsilon_w)}$$

With few exceptions, the R-value does not vary appreciably with strain.[5]

The strain path is nearly linear in the uniaxial and biaxial testings.[6] Consequently, the ratio of principal strains remains constant during deformation. Therefore, the effective stress and strain in uniaxial tension are

$$\sigma_e = \sqrt{\frac{3(R+1)}{2(R+2)}}\sigma_1$$

$$\varepsilon_e = \sqrt{\frac{2(R+2)}{3(R+1)}}\varepsilon_1$$

and effective prestrains in equibiaxial tension is given by

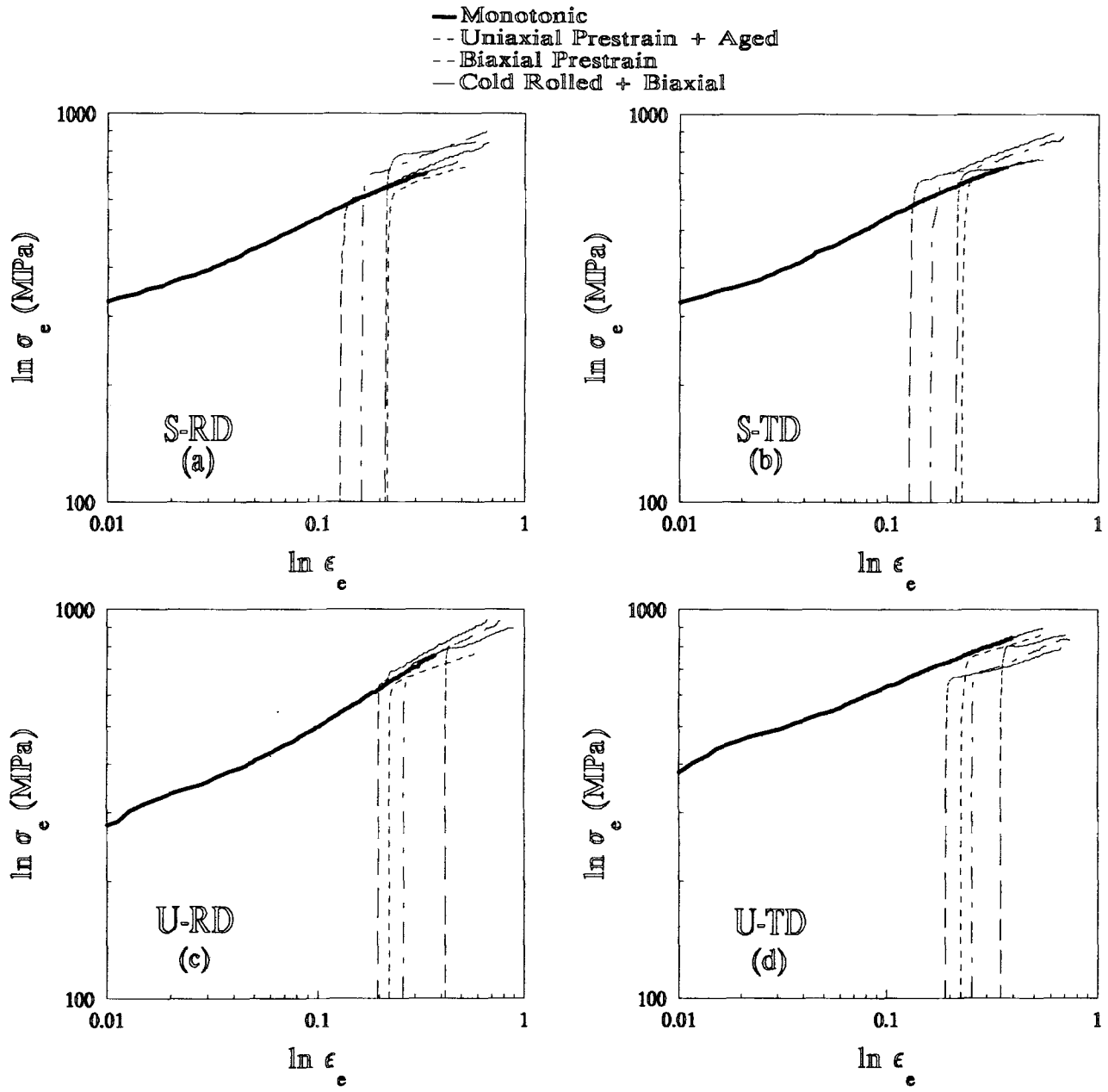

Fig. 2 True stress versus true effective strain for the stabilized (S) and unstabilized (U) sheet steels after the indicated strain path histories. (a) and (c) Tensile samples parallel to the rolling direction. (b) and (d) Samples perpendicular to the rolling direction.

$$\varepsilon_e = \sqrt{\frac{(\bar{R}+2)}{3}}\varepsilon_3$$

where ε_3 is the true thickness strain. The $\bar{R}$-values equal to 1.4 and 1.68 (obtained from private discussion with manufacturers of the examined sheet) were applied to calculate the true effective stresses and strains for unstabilized and stabilized sheet, respectively.

The average slope of the $\sigma_e - \varepsilon_e$ curves were determined by using a linear regression method in very small intervals of 10-point strains. $d\sigma_e / d\varepsilon_e$ versus ε_e curves were smoothed by applying a polynomial regression of either the fourth or fifth order.

3.1 *Stress-Strain Behavior*

The effects of processing history on the stress-strain behavior of the stabilized (S) steel are summarized in Fig. 2(a) and (b) for samples parallel (S-RD, Fig. 2a) and transverse (S-TD, Fig. 2b) to the rolling direction. In addition to the monotonic stress-strain curve, each figure includes data for two samples machined from sheet biaxially stretched to two different strain levels; one sample from cold rolled and biaxially stretched

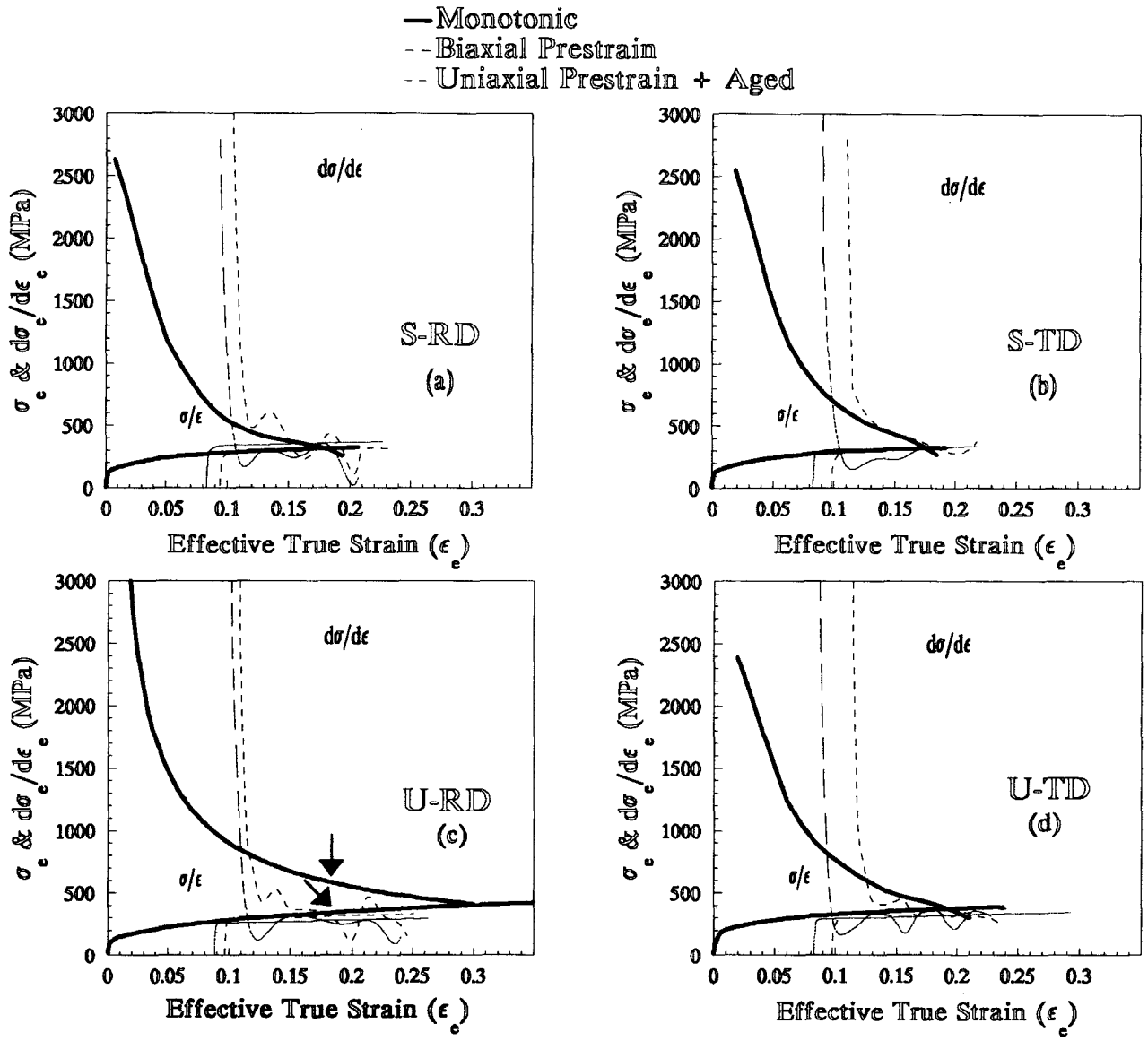

Fig. 3 True strain-hardening rates as a function of true effective strain superimposed on the true stress versus true strain data for a series of stabilized (S) and unstabilized (U) steel samples with the indicated strain histories. (a) and (c) Parallel to the rolling direction. (b) and (d) Perpendicular to the rolling direction. Arrows in (c) indicate that σ-ε and $d\sigma/d\varepsilon$ curves extrapolated to the point of intersection.

sheet, and one sample that was deformed in uniaxial tension and aged. The strain path histories of the samples are summarized in Table 2. The intercepts along the effective strain axis indicate the total restrains for each condition in the first mode of deformation. The uniaxial prestrain and aged material exhibit flow stresses equivalent to the monotonic sample. These comparisons indicate that the tensile properties were unaffected by aging. All of the samples that were prestrained by complex strain paths exhibited flow stresses greater than the monotonic data, except for the unstabilized sheet in the transverse direction (TD). These results illustrate that the instantaneous flow stresses are sensitive to strain history.

As in Fig. 2(a) and (b), Fig. 2(c) and (d) present two sets of uniaxial flow curves, with respect to the rolling direction, for the unstabilized material for the same strain histories discussed above. Again, the total effective strain history is indicated by the intercept on the effective strain axis. Unlike the stabilized steel, all of the flow curves for the unstabilized steel in the rolling direction are not as high as the monotonic data. However, the data for the transverse direction are clearly below the monotonic data. The lower flow stresses after prestraining were not anticipated for sheet steels.[1,7] The Doucet and Natarajan report[3] indicates the lower level of yield at stresses below the expected monotonic level for IF steel, which they used in their experiments. The authors' further detailed crystallographic texture examinations on the unstabilized and stabilized sheet steels, before and after predeformation, revealed the effect of initial texture on the observed behavior.[8]

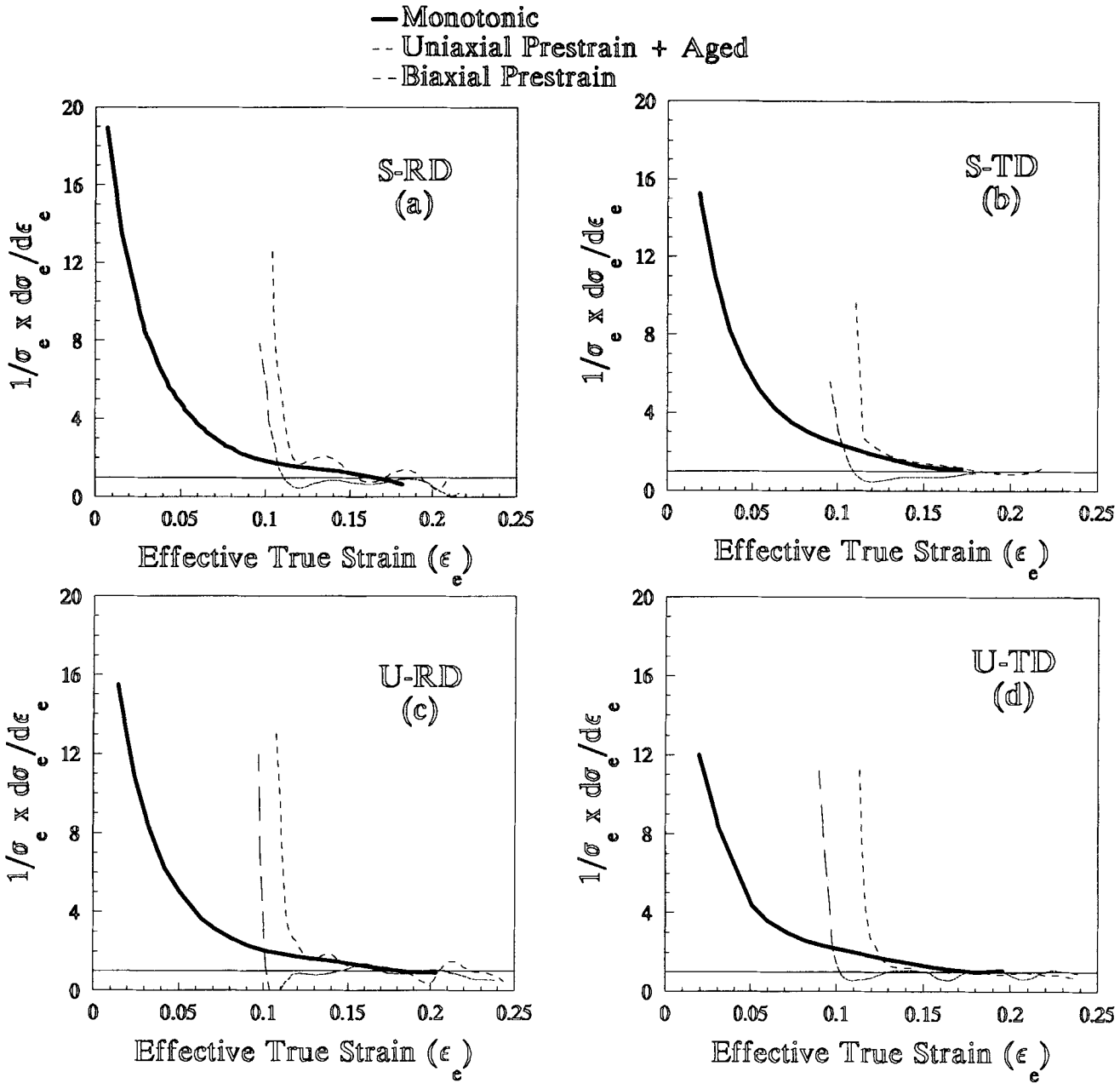

Fig. 4 Normalized work-hardening rate versus effective true strain for the monotonic stabilized (S) and unstabilized (U) steels with indicated histories. (a) and (c) Parallel to the rolling direction. (b) and (d) Perpendicular to the rolling direction. Dotted horizontal lines indicate

3.2 *Strain-Hardening Behavior*

Figure 3 illustrates the effects of strain path on the strain-hardening behavior of stabilized and unstabilized materials, respectively. The strain-hardening data were obtained by determining the slope of the true stress/true strain data shown in Fig. 2. In the earliest stages of plastic deformation after the change in strain path, $d\sigma_e / d\varepsilon_e$ is higher than that at equivalent plastic strains in monotonic deformation. However, $d\sigma_e / d\varepsilon_e$ declines steeply with increasing second-stage straining until $d\sigma_e / d\varepsilon_e$ becomes significantly lower than that developed within a similar range of effective strains in monotonic deformation. The figures indicate that this relative reduction in the hardening rate is transient. At higher levels of effective strain, $d\sigma_e / d\varepsilon_e$ recovers toward that developed at equivalent strains in monotonic deformation. The results, as shown in Fig. 3, do not suggest a significant effect of the rolling direction and stability ratio on the rate of work hardening in the strain ranges that were examined. Figure 4 presents the effect of effective true strain on normalized work-hardening behavior of the ultra-low-carbon sheet steels. The horizontal dotted lines show the uniaxial diffuse instability limit in uniaxial tension described by the following relationship:

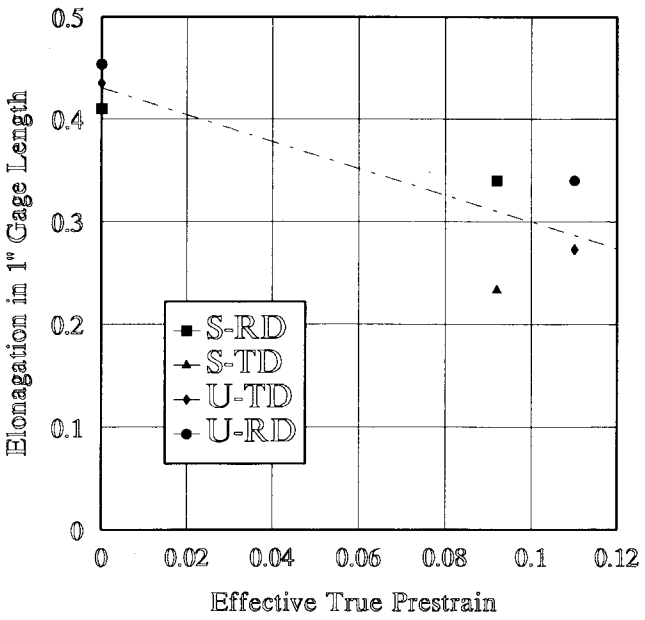

Fig. 5 Presentation of elongation of 1-in. (2.54-cm) gage length specimen versus effective true prestrain by equibiaxial stretching. (S) and (U) are representative of stabilized and unstabilized steels for specimens parallel (RD) and transverse (TD) to rolling directions, respectively.

$$\frac{1}{\sigma_e} \times \frac{d\sigma_e}{d\varepsilon_e} = 1$$

These results clearly illustrate the effect of equibiaxial stretching on the tensile instability of S and U sheet steels. It is concluded that the transient behavior might initiate a diffuse strain localization in the sheet where its levels go below the monotonic hardening rate and the instability limit for uniaxial tension. The initiated instability apparently is a major contribution to the reduction of elongation in uniaxial tension of the prestrained specimens, as shown in Fig. 5.

4. Conclusions

The following conclusions are based on observations of the behavior of stabilized and unstabilized ultra-low-carbon sheet steels in deformation at room temperature. Changes in strain path from equibiaxial stretching to uniaxial tension cause an increase in the initial flow stress relative to the flow stress, with a similar range of strain in continued monotonic deformation on stabilized sheet steels. This phenomenon is more pronounced at the lower level of biaxial prestraining when the tests were carried out at 90 ° to the rolling direction of the specimens. With unstabilized ultra-low-carbon sheet steels, the results indicated that the initial flow stresses decreased with prestraining in equibiaxial or cold rolling and equibiaxial stretching.

Changes in the strain path from equibiaxial stretching to uniaxial tension cause transient changes in the work-hardening rate. In the earlier stages of deformation, there is an increase in work-hardening rate relative to the hardening rates maintained in monotonic deformation. The next mode of transient behavior is reduction in the work-hardening rate toward the monotonic rate of hardening. Both stabilized and unstabilized sheet steels behaved similarly to the change in strain path in the current experiments.

Equibiaxial deformation caused reduction in tensile elongation of the ultra-low-carbon steel sheet. This behavior could be associated with the initiation of diffuse strain localization in the two-stage tests at elongation values much lower than the extension limit in monotonic stretching. In the context of multistage sheet-forming processes, the work-hardening measurements, made in monotonic uniaxial tensile tests, should not be relied upon strongly for use in press forming of sheet steels.

Acknowledgment

This research was sponsored by the National Science Foundation, Engineering Directorate, Industrial University Cooperative Research Centers, under grant No. ECD-9020344 to Southern University, Baton Rouge and its precursors. The authors acknowledge support from the Advanced Steel Processing and Products Research Center (ASPPRC) at the Colorado School of Mines. They are particularly thankful to Professors G. Krauss and D.K. Matlock for invaluable discussion, and would also like to express gratitude to Dr. S.S. Chehl of the Southern University Mechanical Engineering Department for his assistance and Professor S. Nourbakhsh for his review and comments.

References

1. R.H. Wagoner and J.V. Laukonis, Plastic Behavior of Aluminum-Killed Steel Following Plane-Strain Deformation, *Metall. Trans.*, Vol 14A, 1983, p 1487-1495
2. M. Zandrahimi, S. Platias, D. Price, D. Barrett, P.S. Bate, W.T. Roberts, et. al., Effects of Changes in Strain Path on Work Hardening in Cubic Metals, *Metall. Trans.*, Vol 20A, 1989, p 2471-2482
3. A.B. Doucet and R.H. Natarajan, Yielding Behavior of Prestrained Interstitial-Free Steel and 70/30 Brass, *Metall. Trans.*, Vol 5A, 1991, p 393-401
4. B. Taylor, Formability Testing of Sheet Metals, *Metals Handbook*, 9th ed., ASM International, Vol 14, 1988, p 877-899
5. W.F. Hosford and R.M. Caddell, *Metal Forming*, Prentice-Hall, 1983, p 263-273
6. Z. Marciniak, Sheet Metal Forming Limits, *Mechanics of Sheet Metal Forming*, D.P. Koistinen and N.-M. Wang, Ed., Plenum Press, 1978, p 215-235
7. W.B. Hutchinson, R. Arthey, and P. Malmstron, On the Anomalously Low Work-Hardening in Pre-Strained Metals, *Scr. Metall.*, Vol 10, 1976, p 673-675
8. R.A. Mirshams, K.E. Crosby, H.P. Mohamadian, and C.L. Burris, The Influence of Biaxial Stretching on Texture of Ultra Low Carbon (ULC) Sheet Steels, *Scr. Metall. Mater.*, Vol 29(No. 4), 1993, p 433-438.